JOURNAL OF VIROLOGY, June 1994, p. 3512–3526
0022-538X/94/$04.00+0

Vol. 68, No. 6

# Preexisting Nuclear Architecture Defines the Intranuclear Location of Herpesvirus DNA Replication Structures

ANNE DE BRUYN KOPS† AND DAVID M. KNIPE*

*Department of Microbiology and Molecular Genetics, Harvard Medical School, Boston, Massachusetts 02115*

Received 13 December 1993/Accepted 21 February 1994

**Herpes simplex virus DNA replication proteins localize in characteristic patterns corresponding to viral DNA replication structures in the infected cell nucleus. The intranuclear spatial organization of the HSV DNA replication structures and the factors regulating their nuclear location remain to be defined. We have used the HSV ICP8 DNA-binding protein and bromodeoxyuridine labeling as markers for sites of herpesviral DNA synthesis to examine the spatial organization of these structures within the cell nucleus. Confocal microscopy and three-dimensional computer graphics reconstruction of optical series through infected cells indicated that viral DNA replication structures extend through the interior of the cell nucleus and appear to be spatially separate from the nuclear lamina. Examination of viral DNA replication structures in infected, binucleate cells showed similar or virtually identical patterns of DNA replication structures oriented along a twofold axis of symmetry between many of the sister nuclei. These results demonstrate that HSV DNA replication structures are organized in the interior of the nucleus and that their location is defined by preexisting host cell nuclear architecture, probably the internal nuclear matrix.**

Viral replication occurs within defined areas of the host cell called factories or inclusions. These may be located in either the host cell nucleus or the cytoplasm, depending on the site of replication of the virus. Viral DNA replication and encapsidation have been shown to occur within inclusion bodies in the nucleus of cells infected with herpesviruses (17, 30), adenoviruses (33), or parvoviruses (25). Although there is evidence that cell DNA replication occurs at specific sites throughout the interior of the cell nucleus (15), the spatial organization of viral DNA replication structures in the cell nucleus remains undefined. Some evidence supports the idea that viral DNA replication occurs at the periphery of the nucleus (25, 29), while other reports support the idea that replication occurs within the interior of the nucleus (31).

Herpes simplex virus (HSV) encodes seven viral gene products that are required for viral DNA replication (5, 17, 34) and which are sufficient for amplification of DNA containing an HSV origin of replication in transfected cells (4, 36). These viral DNA replication proteins localize to intranuclear structures named replication compartments in infected cells (8, 13, 26–28). These structures colocalize with the major sites of DNA synthesis in infected cells (8, 28); thus, viral DNA synthesis is thought to occur in these structures. In infected cells in which viral DNA synthesis is blocked, several of the viral DNA replication proteins show a punctate distribution in the cell nucleus at sites named prereplicative sites (8, 13, 27). The host cell DNA replication apparatus (8) and specific host cell replication proteins (35) have been shown to colocalize with these structures. Therefore, these patterns seem to reflect the assembly of viral and cellular components required for viral DNA synthesis. These replication structures are dynamic in that the replication proteins rearrange reversibly to give one or the other pattern, depending on the status of viral DNA replication (9, 27). The formation of prereplicative sites and the localization of the HSV DNA polymerase to the prereplicative sites require the HSV ICP8 DNA-binding protein (1, 8). Although one early study indicated that ICP8 may assume a distribution similar to that of prereplicative sites independently of other viral proteins (27), other recent studies have shown that ICP8 shows a diffuse nuclear distribution in the absence of other viral proteins (11). The other viral proteins required for prereplicative site formation have not been defined.

The formation of prereplicative sites and replication compartments in HSV-infected cells provides a useful model system with which to study the mechanisms controlling assembly of functional protein complexes within the cell nucleus and to investigate the possible involvement of the nuclear envelope and/or internal nuclear matrix in the organization of a specific nuclear process. We have compared the three-dimensional spatial organization of HSV DNA replication structures and the nuclear lamina in cultured cells using confocal immunofluorescence microscopy. In addition, we have examined the spatial patterns of replication compartments in the paired nuclei of infected, binucleate cells. We show that the HSV DNA replication structures extend throughout the nuclear interior in a highly ordered arrangement which appears to be independent of the nuclear lamina. Furthermore, we provide evidence that the HSV DNA replication compartments are assembled within a preexisting spatial framework within the cell nucleus.

## MATERIALS AND METHODS

**Cells and virus strains.** African green monkey kidney (CV-1; American Type Culture Collection) cells were used for immunofluorescence studies. Cells were grown in Dulbecco's modified Eagle's medium (Irvine Scientific) containing 10% heat-inactivated fetal calf serum (Gibco), L-glutamine (2 mM;

* Corresponding author. Mailing address: Department of Microbiology and Molecular Genetics, Harvard Medical School, 200 Longwood Ave., Boston, MA 02115. Phone: (617) 432-1934. Fax: (617) 432-0223. Electronic mail address: dknipe@warren.med.harvard.edu.

† Present address: Department of Biochemistry and Biophysics, University of California—San Francisco Medical School, San Francisco, Calif.

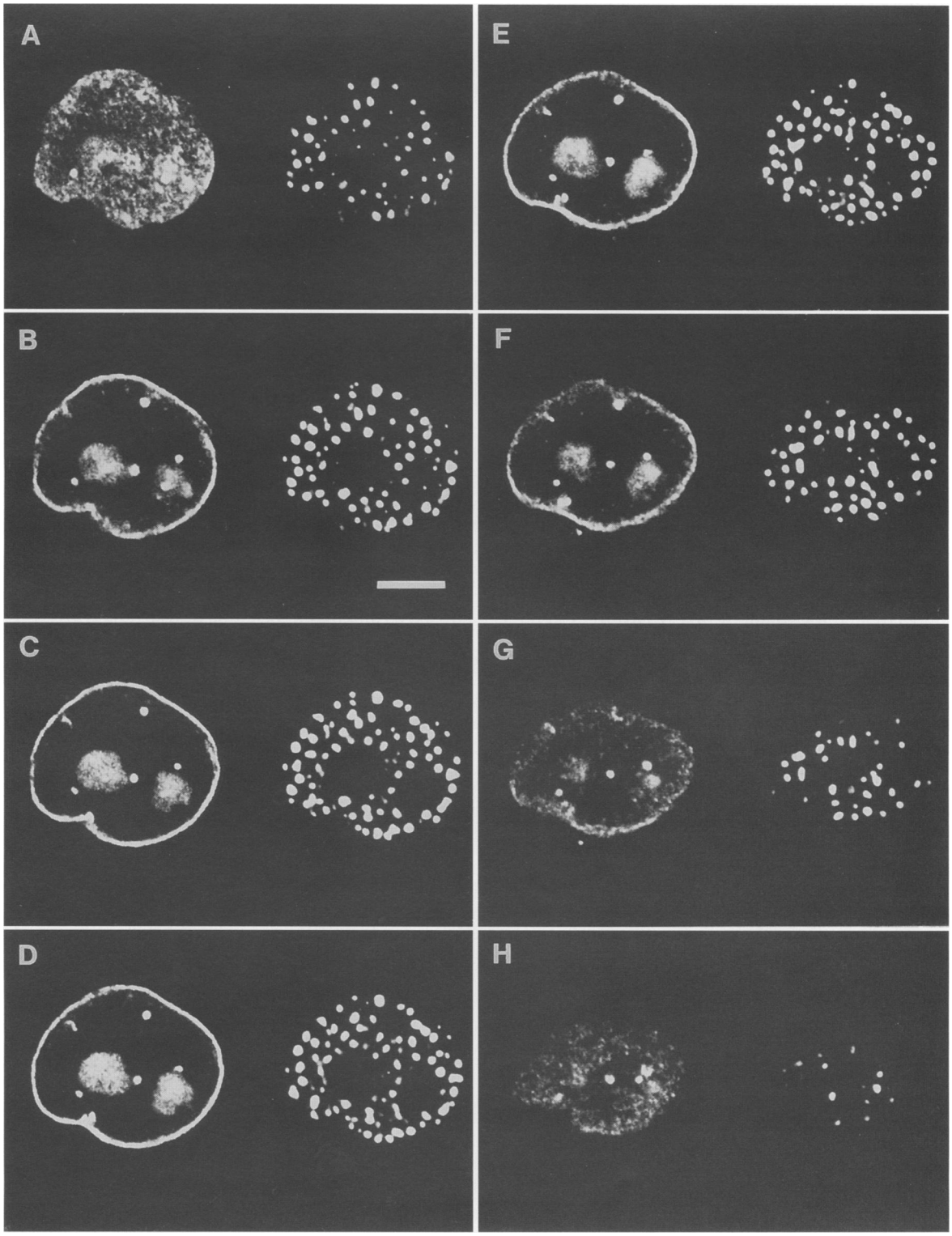


FIG. 1. Optical series comparing the distributions of nuclear lamin and ICP8 in the nuclei of cells infected in the presence of an inhibitor of HSV DNA replication. CV-1 cell monolayers were infected with wild-type HSV-1 in the presence of PAA. Cells were fixed in 2% formaldehyde for 10 min at 5.5 hpi and permeabilized with 0.2% Triton X-100 for 10 min. Cells were stained with a monoclonal antibody specific for lamin proteins and a polyclonal antiserum recognizing ICP8 and then stained with FITC-conjugated goat anti-mouse and biotin-conjugated goat anti-rabbit secondary antibodies. Cells were then stained with Texas red-conjugated avidin. Dual-channel optical sections (focal depth, approximately 0.5 to 0.6 μm) were collected at increments of 0.4 μm. Panels show sequential sections traversing the nucleus from bottom to top. The left half of each panel shows lamin staining, and the right half shows ICP8 staining. Bar, 5 μm.

Flow Laboratories), streptomycin sulfate (Sigma), and penicillin G potassium (Squibb).

The HSV type 1 strains KOS1.1 (16) and macroplaque (MP) (14) were grown and titers were determined as previously described (20). Virus was diluted in cold phosphate-buffered saline (PBS) containing 0.1% glucose and 1.0% heat-inactivated newborn calf serum (Gibco) and adsorbed to CV-1 cell monolayers for 1 h at 37°C. The inoculum was then removed, and medium 199 containing 1% newborn calf serum was added. Infections were carried out at a multiplicity of infection of 20 for all experiments.

**Reagents and antibodies.** Texas red-conjugated avidin (Organon/Teknika), cytochalasin B (Calbiochem), glycerol-gelatin (Sigma), and *p*-phenyldiamine (Sigma) were obtained from the indicated suppliers. The 3-83 rabbit antiserum against ICP8 was described previously (19). The E3 monoclonal antibody recognizing lamin $B_2$ (21) was a gift from Brian Burke. Biotin-conjugated goat anti-rabbit and fluorescein isothiocyanate (FITC)-conjugated goat anti-mouse immunoglobulins were obtained from Cappel.

**Indirect immunofluorescence microscopy.** Cells were grown on coverslips and infected with virus in the presence or absence of 400 μg of sodium phosphonoacetate (PAA) per ml. Cells were fixed for 10 min with 2% formaldehyde in PBS, pH 7.6. The coverslips were rinsed with PBS and then with glass-distilled water, and the cells were permeabilized with acetone for 2 min at −20°C or with 0.2% Triton X-100 at room temperature for 10 min and then rinsed with glass-distilled water. In experiments using bromodeoxyuridine (BrdU) labeling, cells were treated for 10 min with 4 N HCl to expose the incorporated BrdU residues. The cells were washed twice for 5 min with PBS to neutralize the acid. For dual and single antibody staining, 10 μl of PBS containing appropriate dilutions of the primary antibodies was spread on each coverslip. The coverslips were incubated for 30 min at 37°C in a humid chamber. They were then washed three times for 5 min with PBS. Ten microliters of PBS containing diluted goat secondary antibodies was then added to each double-stained coverslip. The coverslips were again incubated at 37°C for 30 min in a humid chamber. Coverslips were washed three times for 5 min with PBS, rinsed with glass-distilled water, and mounted in glycerol-gelatin containing 1.3 mg of *p*-phenyldiamine per ml to retard bleaching. Fluorescent beads (diameter, 1 μm; emission optimum, 540 nm) (Polysciences) were added to the mounting medium for some experiments to assess the apparent size of the fluorescent images from structures of a defined size.

**Confocal microscopy and image analysis.** Standard immunofluorescence and phase-contrast microscopy were performed by using a Zeiss standard microscope with a Plan Neofluar 63× objective lens as described previously (19). Confocal immunofluorescence microscopy (for a review and references, see reference 32) was done with the Bio-Rad MRC-600 confocal imaging system mounted on a Zeiss Axiophot microscope equipped with a 63× Plan Apochromat objective lens. Optical series of infected cells were collected by using the single- and dual-channel functions at stage motor increments of 0.4 or 0.5 μm. Scans were collected with the channel apertures maximally closed. This setting gives an estimated focal depth of approximately 0.5 to 0.6 μm (manufacturer's estimate) when used in combination with a high numerical aperture objective. Series beginning several sections above the nucleus and continuing several sections past the nucleus were collected. All sections showing significant staining were included in the final series.

Texas red and FITC were used as fluorochromes in these studies to optimize dual-channel signal separation. The laser band emission on this system excites the FITC fluorochrome more efficiently than the Texas red fluorochrome. Therefore, Texas red signals were amplified by first staining the cells with goat secondary antibodies conjugated to biotin and then reacting them with Texas red-conjugated avidin. Sixteen-bit images were collected and scaled by a factor of 5 to 10 before being stored as 8-bit images with pixel intensities ranging from 0 to 255 to retain low-intensity information. All images within a series were scaled by the same factor to preserve the relative fluorescence between bright and dim sections. Scale factors were selected such that the brightest intensities were less than 255.

**Computer graphics three-dimensional imaging.** A computer software routine based on the published marching cubes algorithm (23) was used to generate a three-dimensional polygonal data set from the optical series data. The polygons were displayed by using standard computer graphics rendering techniques which employ shadowing and highlighting to produce three-dimensional monochromatic images (10). Rendering was carried out with a Hewlett-Packard/Apollo DN 10000VS graphics workstation by using the GMR3D rendering library.

## RESULTS

We wished to define the intranuclear location of the viral DNA replication structures in cells infected with HSV and, in particular, to ask whether they are localized at the nuclear periphery, possibly in association with the nuclear lamina, or in the nuclear interior. We used confocal immunofluorescence microscopy to obtain a series of optical sections through the nuclei of HSV-infected CV-1 cell monolayers stained with antibodies against ICP8, the viral single-stranded DNA-binding protein, and a cellular nuclear lamin protein. ICP8 has previously been shown to localize to large replication compartments when viral DNA replication is permitted and to more numerous punctate, prereplicative sites when viral DNA replication is blocked during infection with viral DNA polymerase mutants or by the drug PAA (8, 27), which specifically inhibits the HSV DNA polymerase (24). Thus, ICP8 provides a marker for these viral DNA replication structures. The three-dimensional data sets were modeled by using computer graphics reconstructions to generate rendered images, allowing the visualization of replication compartments and prereplicative sites in three dimensions.

**Replication compartment and prereplicative site structures are located in the nuclear interior.** To allow the formation of prereplicative sites or replication compartments, CV-1 cells

FIG. 2. Optical series comparing the images of prereplicative sites and 1-μm-diameter fluorescent beads. Cells were infected, fixed, and permeabilized as described in the legend to Fig. 1 and stained with a polyclonal antiserum recognizing ICP8 followed by FITC-conjugated goat anti-rabbit antibody. Coverslips were mounted in glycerol-gelatin containing fluorescent polystyrene beads with a diameter of 1 μm. Optical sections (approximately 0.5 μm thick) were collected at 0.5-μm increments with the fluorescein channel of the dual-channel filter set used for the experiment shown in Fig. 1. Panels show consecutive sections through a representative cell. Arrows indicate positions of fluorescent beads. Bar, 10 μm.

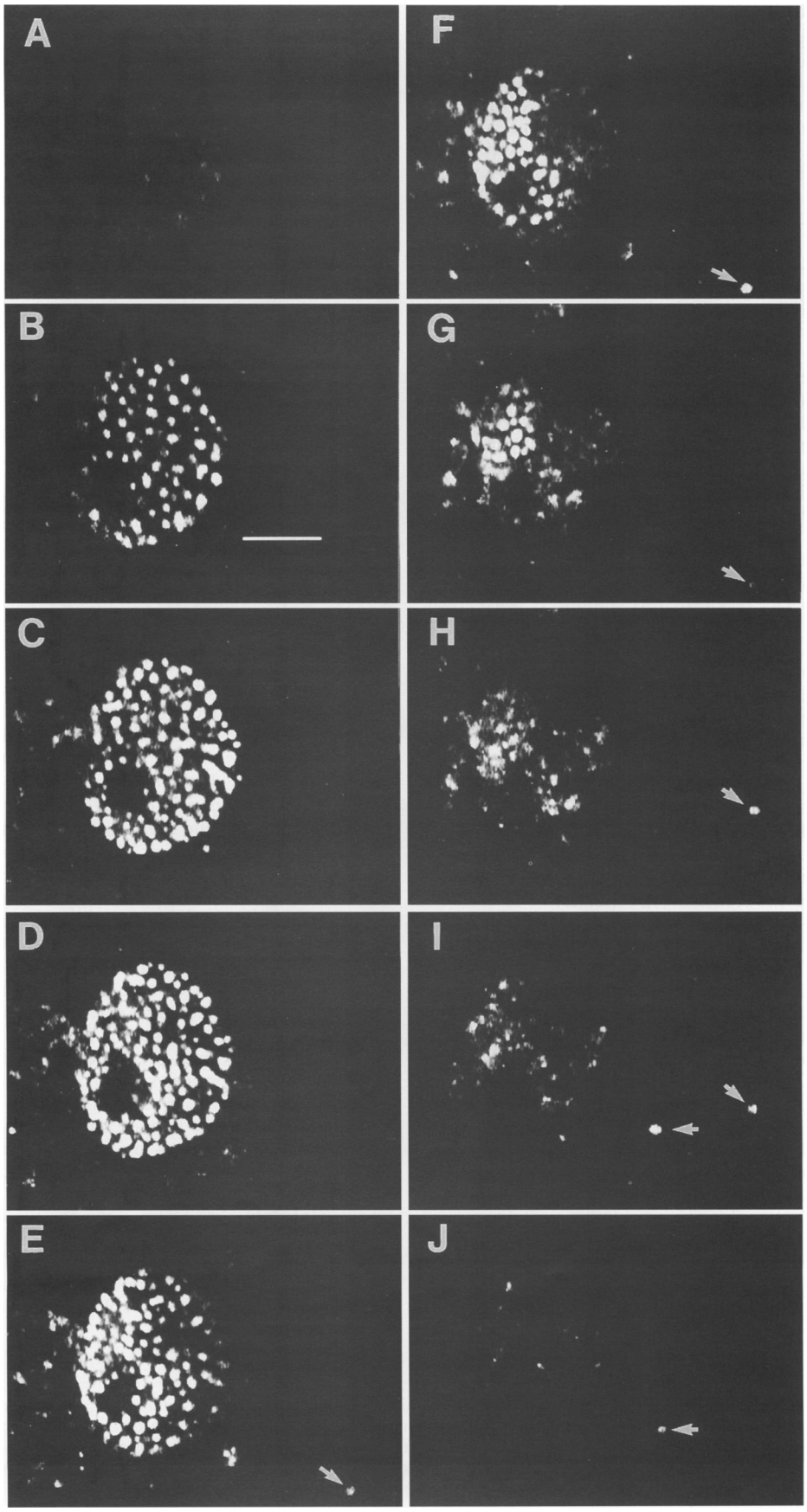
A
F
B
G
C
H
D
I
E
J

were infected with wild-type HSV in the presence or absence of PAA, respectively. Cells were fixed with formaldehyde at 5.5 h postinfection (hpi), permeabilized with Triton X-100, and dual stained for indirect immunofluorescence with a rabbit polyclonal antiserum specific for ICP8 and a mouse monoclonal antibody recognizing a nuclear lamin protein. Data sets consisting of serial optical sections through infected nuclei were obtained by using a confocal microscope. Sections were collected at 0.4-μm increments with an estimated focal depth of approximately 0.5 to 0.6 μm. Double-channel images were collected, allowing the simultaneous recording of lamin and ICP8 staining at each focal position. The simultaneous collection of the two images eliminated alignment errors possible if series of lamin and ICP8 staining in the same nucleus had been collected separately.

A representative series of optical sections through the nucleus of a cell infected in the presence of PAA to inhibit viral DNA replication showed a pattern of prereplicative sites which extended through all sections (Fig. 1, right half of each panel). In contrast, lamin staining (Fig. 1, left half of each panel) was observed as rim staining in the middle sections of the series (panels C through E), staining the entire face of the nucleus only at the outermost sections (panels A and H). This pattern was consistent with the established location of lamin proteins adjacent to the nuclear envelope. Some cells also showed staining of internal structures, possibly nucleoli, with the antilamin antibody. The origin of this staining is not known. The presence of ICP8 staining in the interior sections (Fig. 1, panels B through F) indicates that prereplicative sites extended through the interior of the nucleus and were not restricted to the vicinity of the lamina at the nuclear periphery. The same ICP8 pattern was observed when fluorescein-conjugated secondary antibody was used to detect ICP8 antibody (9). Confocal microscopy studies of infected Vero cells also demonstrated prereplicative sites throughout the nucleus (9). Although we cannot completely exclude the possibility of lateral connections between prereplicative sites, we have never observed significant staining indicative of such connections in standard immunofluorescence micrographs of whole cells or cryosections or in confocal microscopy images.

The nuclei of CV-1 cells have been estimated to be 3 to 4 μm thick on the basis of measurements from electron micrographs (6). Consistent with this, confocal series collected through nuclei at 0.4-μm increments routinely contained 8 to 10 sections (Fig. 1 and 2). The thickness of the optical sections was estimated to be 0.5 to 0.6 μm on the basis of manufacturer estimates of the focal depth obtained with the narrowest possible aperture. One-micrometer-diameter fluorescent beads included in the mounting medium were visible in only two to three sections (Fig. 2, arrows), indicating that this estimate was reasonable and that potential point source distortion in the *z* axis (12) was not likely to be a significant problem in examining large (≥1-μm) structures. In addition, optical sections through nuclei stained with antibodies against a lamin protein showed different staining patterns in adjacent sections (Fig. 1, compare panels A and B), with different diameters delineated by the lamin rim staining in each section. This would not have been observed if the sections had been thicker. For example, if sections were 0.8 μm thick, adjacent sections would be expected to have shown overlapping signal, and lamin antibody staining of the face of the nucleus would be expected for both panels A and B in Fig. 1.

Serial optical sections through the nucleus of a cell infected in the absence of PAA, conditions allowing viral DNA replication, revealed that replication compartments were also present in consecutive sections spanning the interior of the nucleus (Fig. 3, right half of each panel). This was markedly different from the lamin staining in these cells (Fig. 3, left half of each panel) and demonstrated that replication compartments, like prereplicative sites, extend through the nuclear interior. Although measurements of actual distances would not be accurate, the separation between the replication compartments and the lamin staining appeared to be considerable, making direct contact between the replication compartments and the nuclear lamina at the nuclear edges unlikely. For example, ICP8 staining was absent in the first couple of sections at the top and bottom of the nucleus, where lamin staining across the nucleus is evident (Fig. 3A, B, I, and J). In addition, when the lamin and ICP8 images from sections in the middle of the series were superimposed (Fig. 4), the replication compartments appeared to be separated from the lamina. While we cannot rule out connections between these structures not visible at this level of resolution, these observations make extensive direct contact between replication compartments and the nuclear lamina unlikely.

**Prereplicative sites represent large viral structures within the nucleus.** The size of individual prereplicative sites is not known. Two-dimensional immunofluorescence images are consistent with *x* and *y* dimensions on the order of 1 to 2 μm but give no information regarding the size of these structures in three dimensions. With the optical sections through prereplicative sites, individual sites appeared to be located in approximately the same position in several consecutive sections (Fig. 1), suggesting that the sites may be quite large. In experiments in which fluorescent beads (diameter, 1 μm) were included in the mounting medium, optical series collected at 0.5-μm increments revealed the beads in two to three adjacent sections (Fig. 2), as expected for a particle of this size. In contrast, prereplicative sites were apparent in five to six sections in the same series, with individual sites appearing in most or all sections. This suggested that individual or clusters of prereplicative sites are quite large, extending as much as 2 μm in the *z* dimension.

Although individual prereplicative sites appear to extend through several optical sections, it was difficult to evaluate their precise position by eye. To confirm that individual sites were superimposable in consecutive sections, we modeled the optical series data sets using three-dimensional computer graphics imaging. A computer program based on the marching cubes algorithm (23) was used to generate a three-dimensional polygonal data set. These polygons were then rendered by using standard computer graphics techniques, thereby facilitating the visualization of prereplicative sites in three dimensions. By this approach, continuous smooth structures would be expected if individual prereplicative sites extended through

FIG. 3. Optical series comparing the distribution of ICP8 in replication compartments with that of nuclear lamin. CV-1 cells were infected with wild-type HSV in the absence of PAA to allow viral DNA replication and replication compartment formation. At 5.5 hpi, cells were fixed and stained with antisera recognizing ICP8 and an antibody specific for lamin proteins, as described in the legend to Fig. 1. Dual-channel optical sections (focal depth, approximately 0.5 to 0.6 μm) were collected at increments of 0.4 μm. Panels show sequential sections traversing the nucleus from bottom to top. The left half of each panel shows lamin staining, and the right half shows ICP8 staining. Bar, 5 μm.

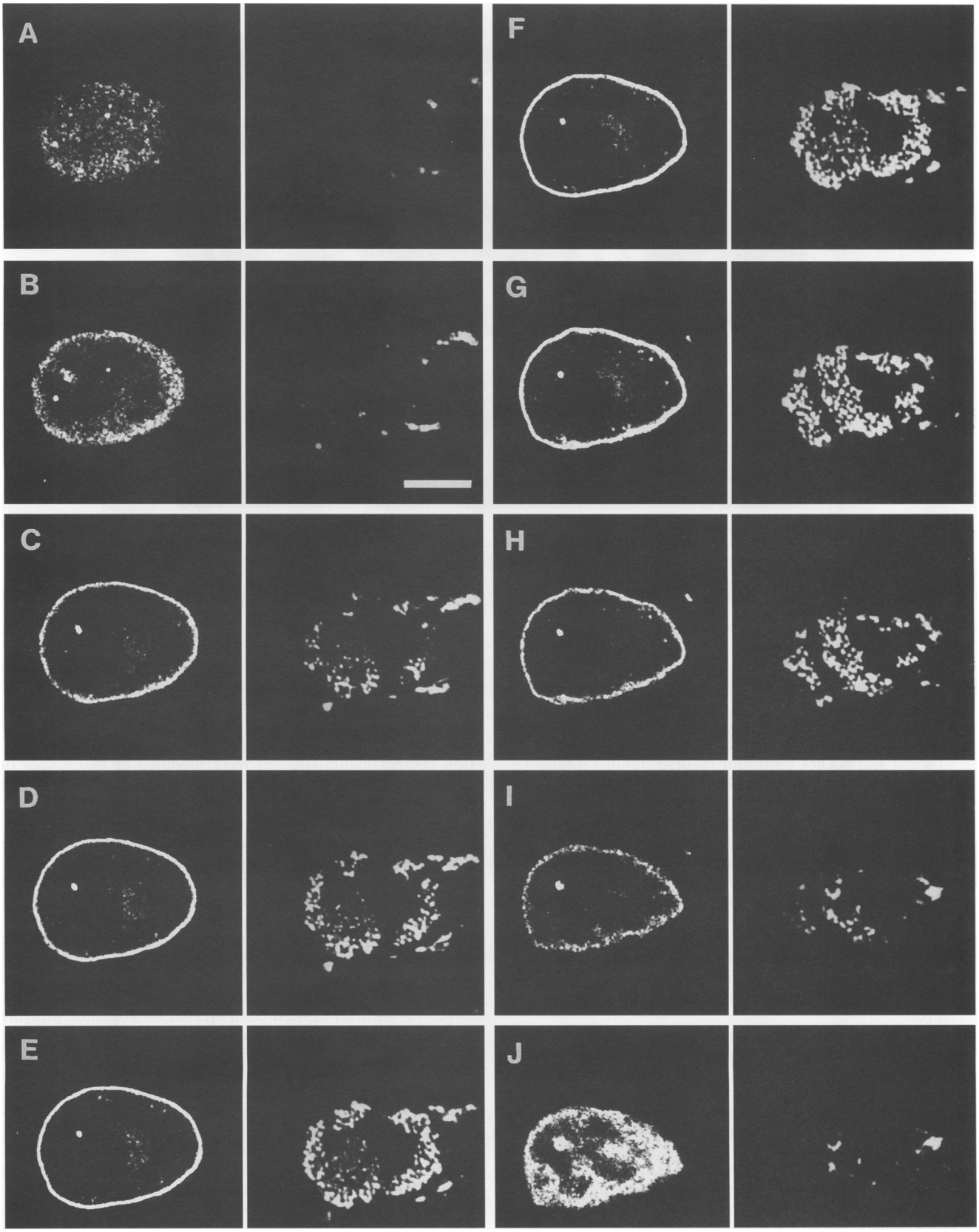
A
F
B
G
C
H
D
I
E
J

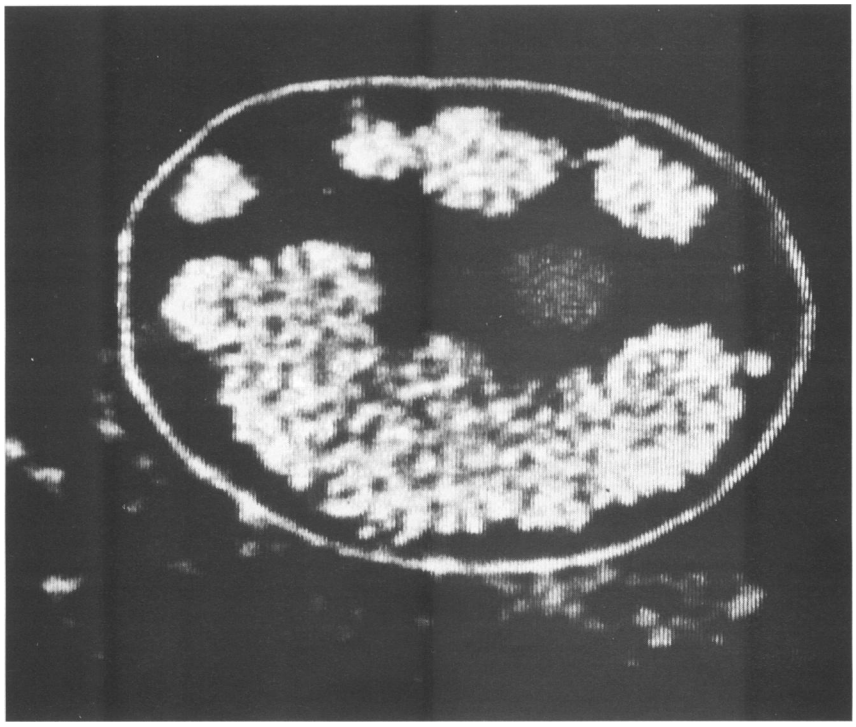

FIG. 4. Merged images of lamin staining and replication compartments from optical sections. Cells were infected with HSV and prepared for immunofluorescence staining with an antibody specific for a lamin protein and antisera specific for ICP8, as described in the legend to Fig. 3. Optical series through the nuclei were collected with a confocal microscope, and images from the middle of the series of optical sections were merged to give a composite image of lamin and ICP8 staining.

consecutive sections, while irregular shapes would be obtained if separate, partially overlapping sites were superimposed.

The data sets were modeled at two angles of rotation by using contouring at a pixel intensity which defined the boundaries of the individual sites. Thus, no pixel information was lost from the prereplicative sites (Fig. 5). In these images, differences in color intensity were used to render the images three dimensional and do not represent relative staining intensities at different positions. The modeled images revealed continuous smooth structures extending approximately 2 μm in the *z* axis, as expected if the prereplicative sites were large structures. The observation that individual prereplicative sites occupy twice as many optical sections as 1-μm-diameter fluorescent beads (see above) argues that the apparent 2-μm dimension in the *z* axis is not merely the result of potential point source distortion but that the prereplicative sites are, in fact, large structures. Although the structures appear elongated in the modeled images, this shape may reflect distortion in the model resulting from higher resolution in the *x* and *y* axes than in the *z* axis rather than the actual shape of the structures.

Because the optical sections constituting the data sets overlapped slightly (focal depth, 0.5 μm; increments, 0.4 μm), there is potential for the modeling to represent individual structures that are separated by small distances in the *z* axis (0.1 μm) as a single continuous structure. Therefore, we cannot rule out the possibility of breaks in the structure. However, we feel that the simplest explanation for the types of images obtained is that individual prereplicative sites or multisite clusters extend for as much as 2 μm through the interior of the nucleus. The large size and regular appearance of the prereplicative sites argue for a high level of spatial organization in the nuclear interior.

The data sets of series through replication compartments were also modeled with two different pixel intensity levels. In one case, all pixel intensities falling within the general area of the replication compartments in each section were used to generate three-dimensional images of the entire compartments at two angles of rotation (Fig. 6). In the second case, the pixel intensities defining the bright foci observed within the replication compartments (Fig. 3) were modeled at two angles of rotation to highlight the greatest concentrations of ICP8 within the compartments (Fig. 7).

The images of the replication compartments (Fig. 6) showed large structures that extended continuously through the nucleus. The images modeling the brightest ICP8 staining (Fig. 7) revealed foci of staining within the compartments reminiscent of the three-dimensional prereplicative site pattern (Fig. 5). Previous studies (8) of the formation of prereplicative sites and replication compartments showed that both the prereplicative site and replication compartment patterns begin with a few foci of staining at early times after infection and diverge as more foci form (in the case of prereplicative sites) or the foci become larger (as with replication compartments). Together with the finding that these patterns are reversible (27), these observations argued for a relationship between the two patterns. These findings raise the intriguing possibility that the replication compartments represent prereplicative sites regrouped into large viral replication compartments when viral DNA replication is ongoing.

**ICP8-containing structures within replication compartments represent the actual sites of DNA replication in infected cells.** The optical series and three-dimensional reconstructions of ICP8 staining clearly show that a protein present in the replication compartments and required for viral DNA synthesis is localized in highly ordered structures in the interior of the

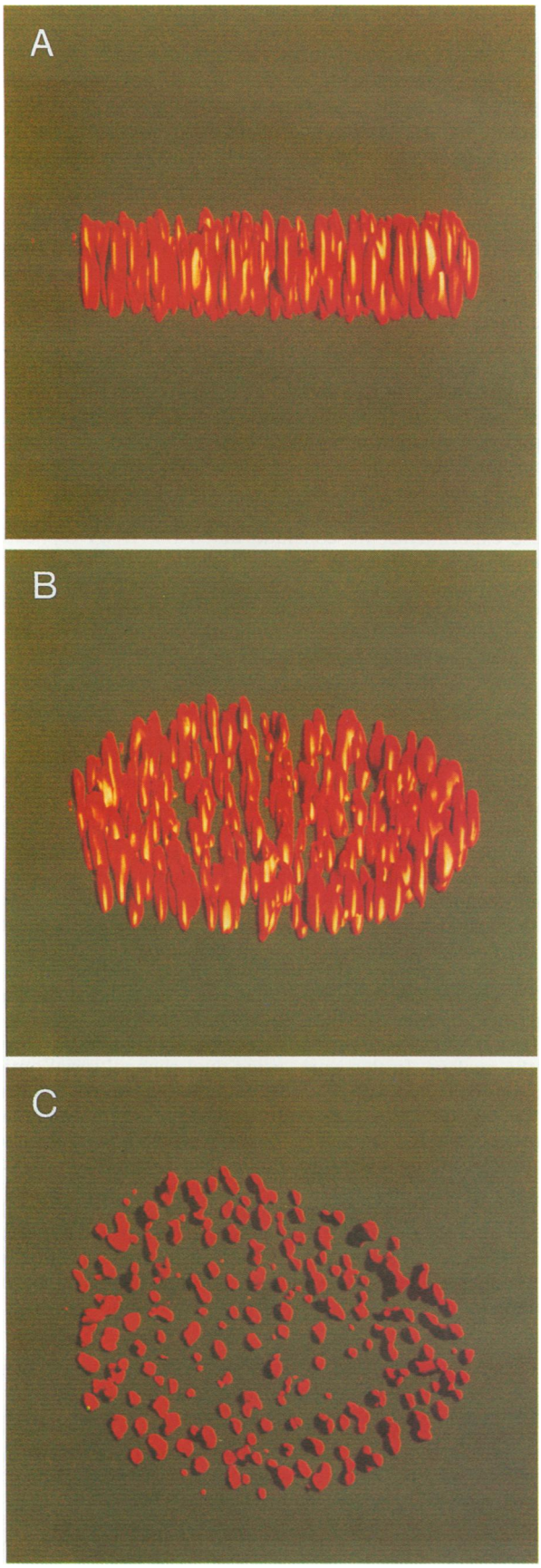


cell nucleus. Using BrdU staining and standard two-dimensional immunofluorescence microscopy, we have shown previously that the replication compartments are the sites of viral DNA synthesis (8). In addition to its role in HSV DNA replication, ICP8 plays a role in other aspects of viral infection. To determine if the three-dimensional distribution of ICP8 in replication compartments corresponded to the location of DNA replication, we collected dual-channel optical series through infected cells pulse-labeled with BrdU and double stained with antibodies against ICP8 and BrdU. The use of dual channels to collect the ICP8 and BrdU images simultaneously eliminates the need to align the images, therefore avoiding alignment artifacts. BrdU staining was localized at discrete foci which coincided with the ICP8 foci within the replication compartments (Fig. 8). Thus, the structures observed within the replication compartments are the sites of DNA replication throughout the nucleus of the infected cell.

**Intranuclear location of HSV replication compartments depends upon preexisting spatial architecture in the nucleus.** The results described above indicated that HSV DNA replication structures are large structures located in the interior of the infected cell nuclei. We wished to determine if the location of these structures was random or if the structures were assembled at specific locations in the cell nucleus. We reasoned that if they were assembled at specific sites, the patterns might be similar in paired nuclei of binucleate cells on the basis of reports that nuclei of newly divided cells show symmetrical distributions of nucleoli and chromosomes (reviewed in reference 22).

To test this possibility, we examined the distribution of HSV replication compartments in binucleate cells following infection with wild-type virus. Binucleate CV-1 cells arose spontaneously in our cell cultures at a frequency of approximately 5%, and HSV infection did not affect this frequency (9). HSV-infected cells were stained with a polyclonal ICP8 antiserum, and the replication compartments in random binucleate cells were examined. Similar or virtually identical numbers and shapes of replication compartments were observed in the paired nuclei of binucleate cells (Fig. 9A through D and F through I). These patterns often appeared to be mirror images of one another, oriented along a twofold axis of symmetry running between the nuclei.

To increase the proportion of binucleate cells, we treated cells overnight with 0.5 μg of cytochalasin B per ml to disrupt cytokinesis. When this was done, it was possible to observe several binucleate cells showing similar patterns of replication compartments in any given field (Fig. 9E and J). The proportion of binucleate cells which showed similar patterns was somewhat variable, with as many as one-half to two-thirds being similar in randomly selected fields for several separate experiments. The criteria for scoring paired nuclei as similar were the number, shape, and position of the replication compartments.

FIG. 5. Three-dimensional computer graphics reconstruction of prereplicative sites. A computer graphics algorithm was used to calculate polygon values from data sets of optical series collected at 0.4-μm increments through cells infected in the presence of PAA and stained with antisera against ICP8. The polygons were modeled with an Apollo/Hewlett-Packard DN10000 workstation by using standard computer graphics rendering techniques and the Apollo/Hewlett-Packard GMR3D rendering library. Panel A shows an image of a nucleus viewed from the side, and panel B shows the image viewed from the top at an oblique angle. Panel C shows the image viewed from the top.

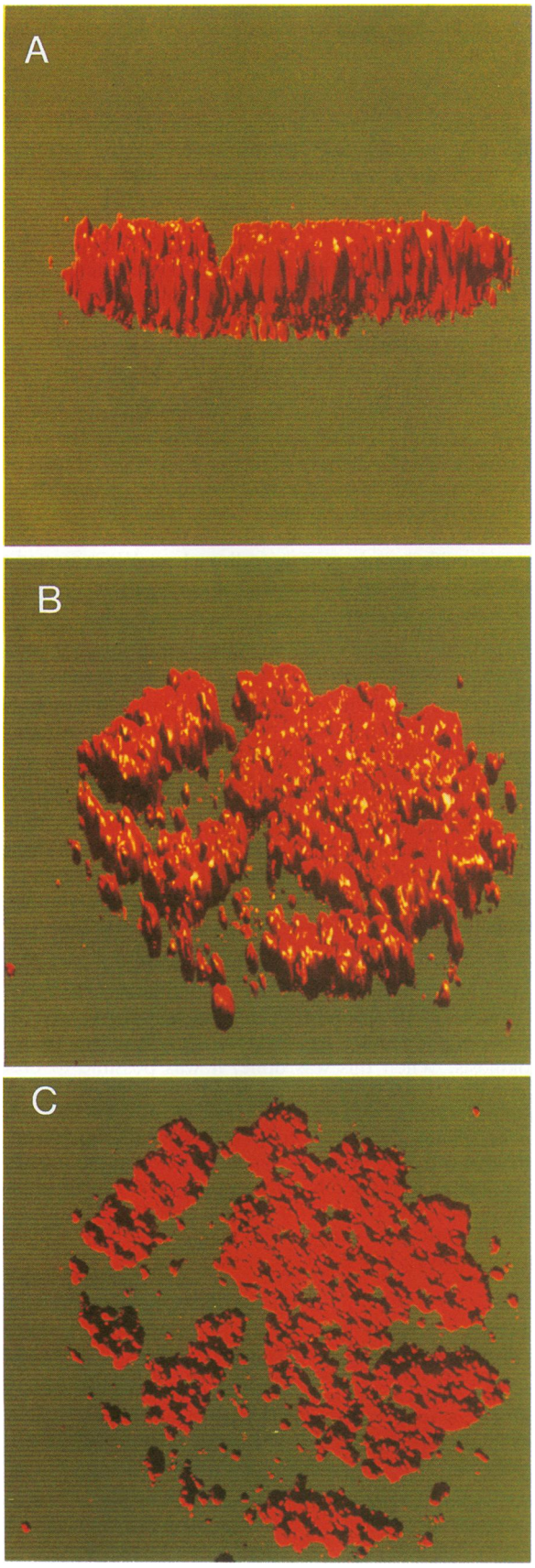


The large number of similar or identical patterns in the paired nuclei was particularly remarkable considering that the likely divergence of spatial patterns over time (22) and rotation of daughter nuclei with respect to one another would be expected to result in dissimilar patterns in some cells. In general, the greatest similarity between viral patterns was observed in nuclei which remained adjacent to one another and retained similar size and overall shape.

The similarity of replication compartments observed in binucleate cells was much greater than that in unrelated nuclei selected at random. For two reasons, this similarity was probably not the result of cells becoming binucleate during infection. First, infection with wild-type HSV did not increase the number of binucleate cells in the population, as described above. Second, infection with a syncytial HSV mutant which causes fusion of cells yielded multinucleated cells with dissimilar patterns of replication compartments (Fig. 10). On this basis, we believe that cells showing paired nuclei with similar replication compartments were binucleate prior to infection. Therefore, the duplication of replication compartment patterns in the daughter nuclei reflected preexisting nuclear spatial arrangements conserved during nuclear division. From these experiments, we conclude that HSV DNA replication proteins are localized to specific regions in the infected nucleus. This may represent targeting of the HSV proteins to specific cell structures; alternatively, viral proteins may localize to areas where formation of replication compartments is not impeded by existing host structures.

## DISCUSSION

There is increasing evidence that nuclear components are localized to specific locations in the cell nucleus (recently reviewed in references 2 and 3). However, in few cases is it known where the structures are located, in particular, whether the structures are at the periphery or in the interior of the nucleus. In addition, whether the structures are located randomly or located at specific sites is not known. In this work, we have shown that HSV DNA replication structures are located in the interior of the nucleus, with little apparent contact with the nuclear envelope. Furthermore, the location of the viral DNA replication structures appears to be defined by some aspect of the preexisting organization of the host cell nucleus.

**HSV DNA replication structures extend through the interior of the nucleus.** In this work, using dual-channel serial optical sections collected with a confocal immunofluorescence microscope, we observed that both replication compartment and prereplicative structures are apparent through several optical sections from the interior of the nucleus. Comparison of these images with those of fluorescent beads of 1-μm diameter indicated that the prereplicative sites were apparent through a depth of approximately 2 μm in the nuclear interior. This is in sharp contrast to the nuclear rim staining observed with lamin antibody staining. Although the borders of the structures cannot be defined accurately from immunofluorescence im-

FIG. 6. Three-dimensional computer graphics reconstructions of replication compartments. Optical series data sets from cells infected in the absence of PAA were collected and modeled by using computer graphics as described in the legend to Fig. 5. Images were contoured at a pixel intensity level such that all staining falling within replication compartments was modeled. Panel A shows an image viewed from the side, and panel B shows an image viewed from the top at an oblique angle. Panel C shows the image viewed from the top.

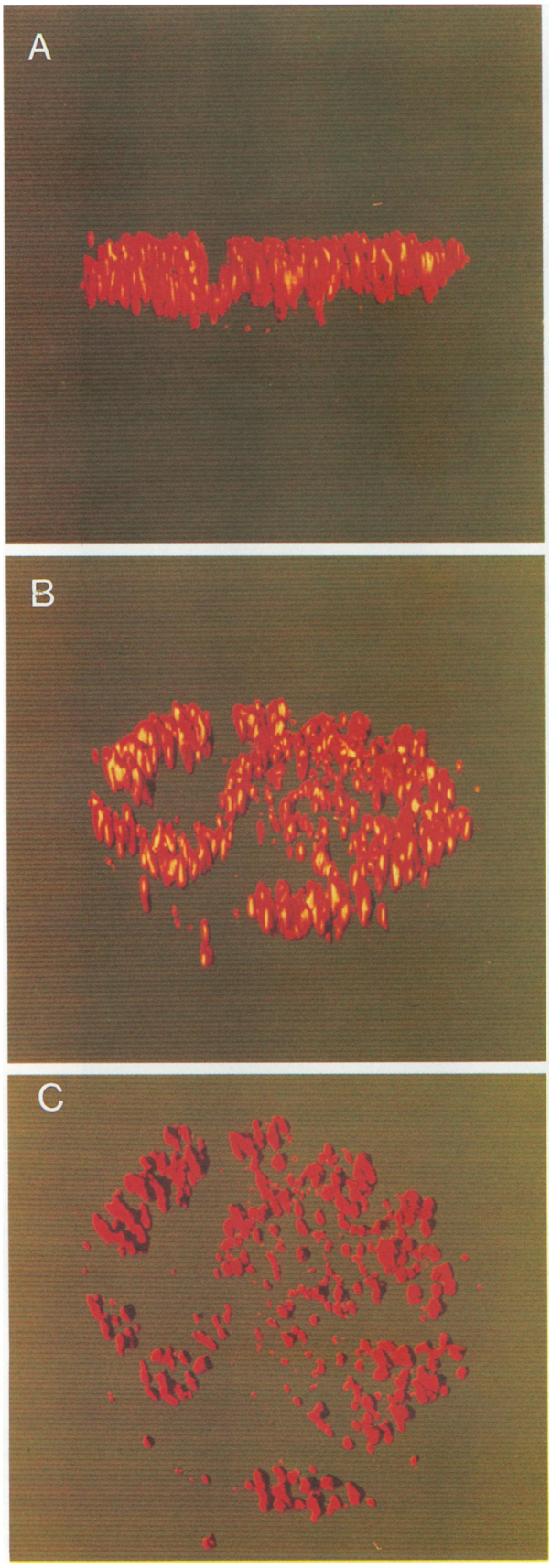


ages, a clear separation between replication compartments and the nuclear lamina is visible in the lateral dimensions of individual sections. This makes extensive physical connection between the viral structures and the nuclear lamina unlikely. In the case of replication compartments, a separation in the vertical dimension is also indicated by the fact that lamin surface staining is visible in sections where no ICP8 staining is evident. At present, we cannot rule out finer connections between the lamina and these structures not visible at the present level of resolution or the possibility that these structures are linked indirectly to the lamina by way of connections with other nuclear components. However, it appears that the viral replication compartments and prereplicative structures are organized in the nuclear interior and are not localized to a peripheral subnuclear compartment. This is consistent with electron microscopic data (7, 31) and light microscopic evidence (28) showing that the host cell chromatin is displaced to the periphery of the host cell nucleus or "marginated" in cells infected with HSV (18). The localization of viral DNA replication compartments in an internal rather than a peripheral nuclear compartment is similar to that reported recently for RNA metabolism (3) and consistent with an emerging view of the nuclear interior as highly organized.

Computer modeling of confocal optical data sets facilitated visualization of HSV DNA replication structures in three dimensions. Prereplicative sites appeared as large structures organized in the nuclear interior. The individual sites appear to be as much as 2 μm deep in the *z* axis, indicating that they extend through much of the depth of the nucleus (estimated to be 3 to 4 μm). The large size and regular arrangement of prereplicative sites in the nuclear interior argue for a high level of internal nuclear organization. Previous studies indicated that ICP8 localized to prereplicative sites fractionating with the nuclear matrix (27). In addition, it was demonstrated that formation of prereplicative sites requires functional ICP8 (8). Taken together with these findings, the ordered arrangement of prereplicative sites in the nuclear interior is consistent with the possibility that ICP8 plays a role in organizing these structures by interacting with a cellular, structural nuclear framework and with viral DNA replication proteins and/or with multiple viral DNA replication proteins.

Three-dimensional image reconstructions indicate that replication compartments are also large structures organized in the nuclear interior. In addition, the images generated from pixel intensity ranges defining the bright foci within the compartments revealed structures resembling prereplicative sites. These foci corresponded to DNA replication sites labeled with BrdU, indicating that there are discrete locations within the replication compartments where DNA replication is concentrated. The distributions of certain HSV transcriptional regulatory proteins, as well as that of the major capsid protein, have been shown to overlap with ICP8 staining in replication compartments (9, 19). Thus, replication compartments may represent general viral replication domains, and the grouping together of components required for different viral processes,

FIG. 7. Three-dimensional computer graphics reconstructions of ICP8 foci within replication compartments. Optical data sets through replication compartments were collected and modeled as described for Fig. 6, except that images were contoured at an intensity level defining the bright foci within replication compartments. Panel A shows an image viewed from the side, and panel B shows an image viewed from the top at an oblique angle. Panel C shows the image viewed from the top.

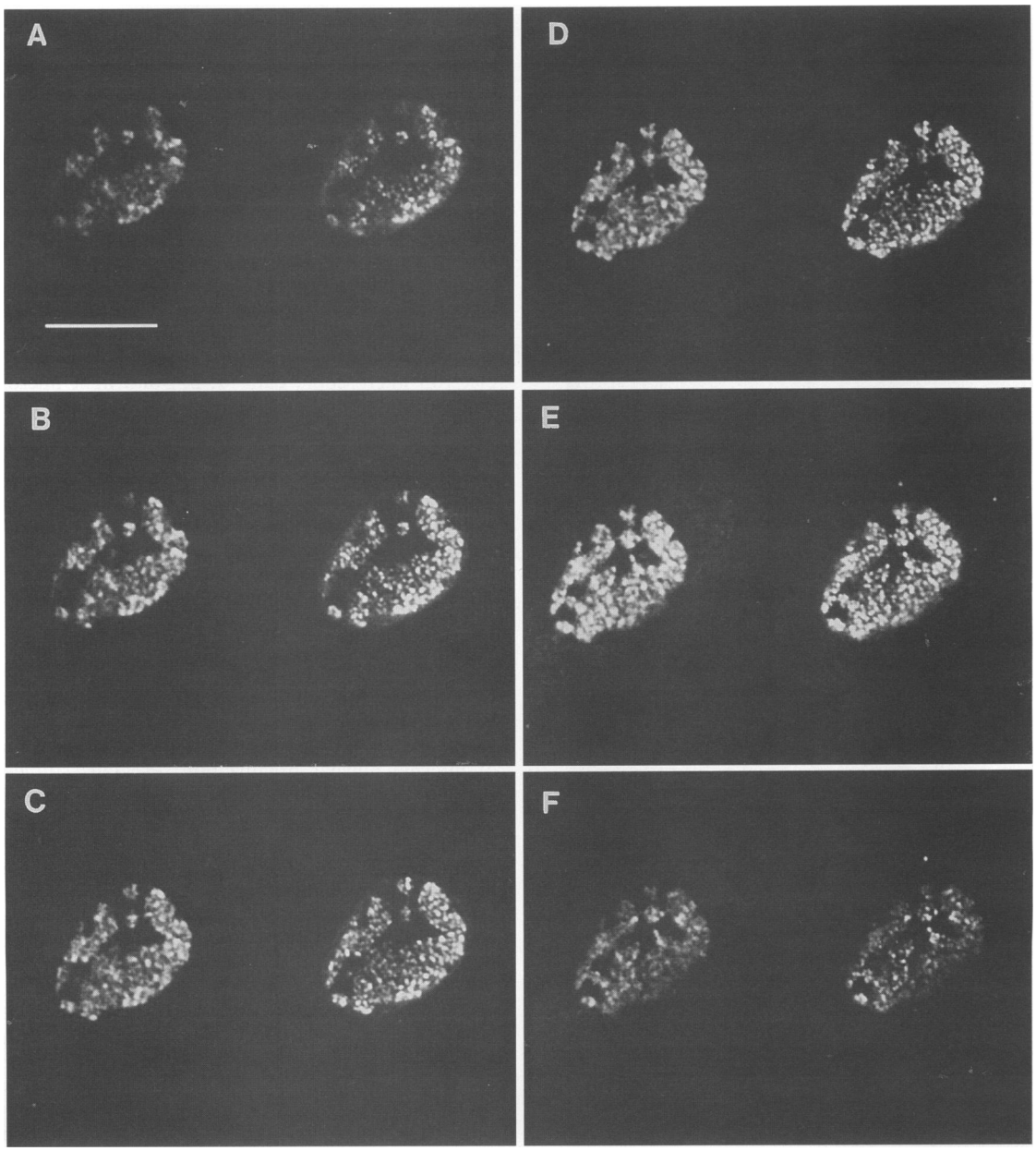


FIG. 8. Optical series comparing the three-dimensional distributions of ICP8 and BrdU labeling in infected cells. CV-1 cells grown on coverslips were infected with HSV and pulse-labeled with 10 μM BrdU starting at 5.25 hpi. The cells were fixed in 2% formaldehyde for 10 min at 5.5 hpi, permeabilized with 0.2% Triton X-100 for 10 min, and then treated with 4 N HCl for 10 min. They were then stained with the 3-83 polyclonal antisera specific for ICP8 and a monoclonal antibody specific for BrdU. The cells were then stained with FITC-conjugated goat anti-rabbit and biotin-conjugated goat anti-mouse secondary antibodies followed by Texas red-conjugated avidin. Series of dual-channel optical sections (focal depth, approximately 0.5 to 0.6 μm) were collected at increments of 0.4 μm by using the confocal microscopy system. Panels show a continuous optical series traversing the nucleus from bottom to top. The left image in each panel shows BrdU staining, and the right image shows ICP8 staining. Images were mapped by a pseudocolor routine resulting in the assignment of black, grey, and white in order of increasing intensity to ranges of pixel intensities. Bar, 5 μm.

FIG. 9. Replication compartments in paired nuclei of binucleate cells. CV-1 cell monolayers were infected with wild-type HSV in the absence of PAA. Cells were fixed with 2% formaldehyde for 10 min at 6 hpi and permeabilized for 10 min with 0.2% Triton X-100. Cells were stained with the 3-83 polyclonal antisera recognizing ICP8 followed by an FITC-conjugated goat anti-rabbit secondary antibody. Panels A through D and F through I show phase contrast (left image) and immunofluorescence (right image) micrographs of individual binucleate cells. Panels E and J show cells treated overnight with cytochalasin B (0.5 μg/ml) to increase the frequency of binucleate cells. Arrows indicate a twofold axis of symmetry. The bar in panel A (for panels A through D and F through I) equals 10 μm, and the bar in panel E (for panels E and J) equals 20 μm.

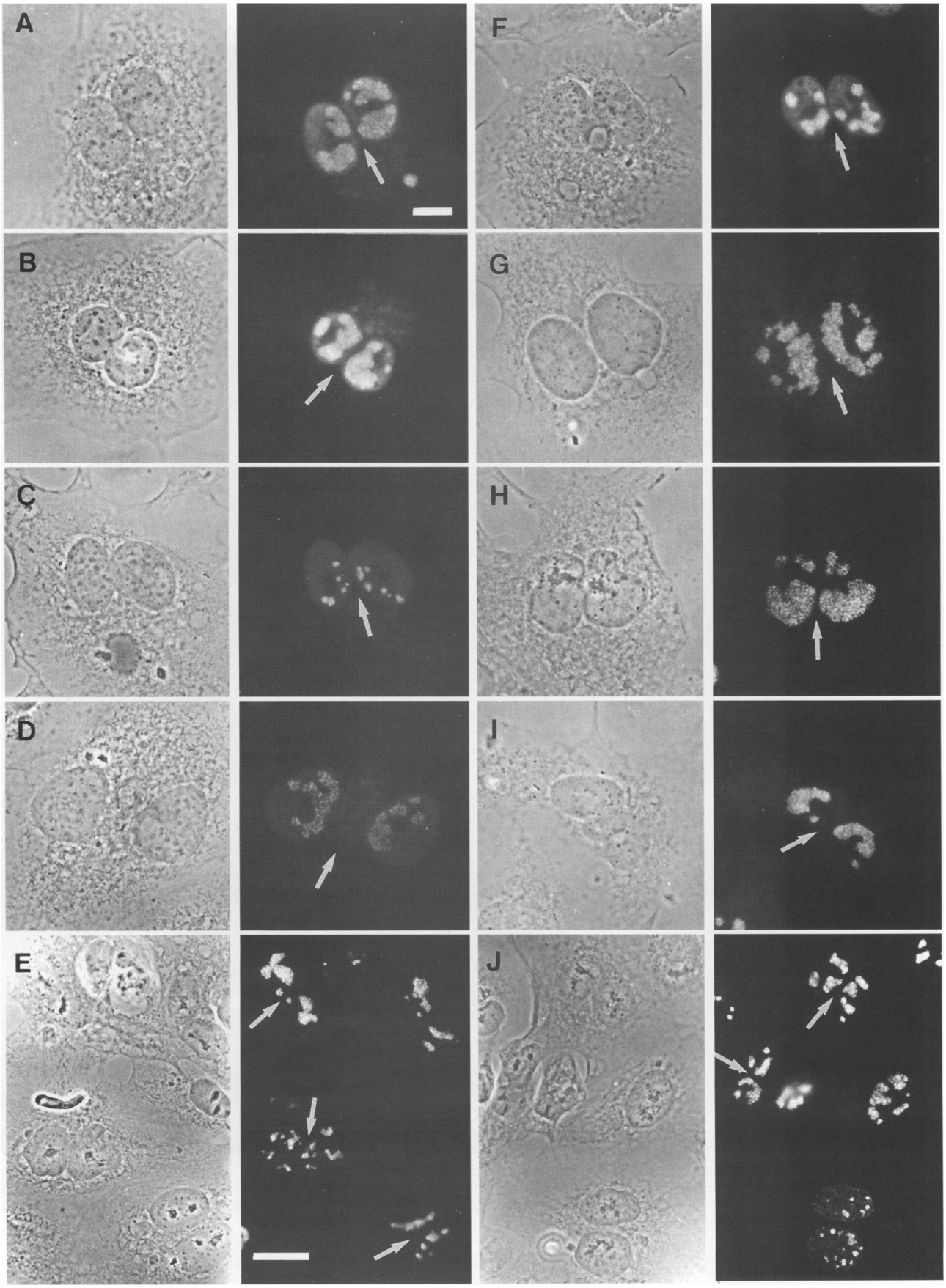
A
B
C
D
E
F
G
H
I
J

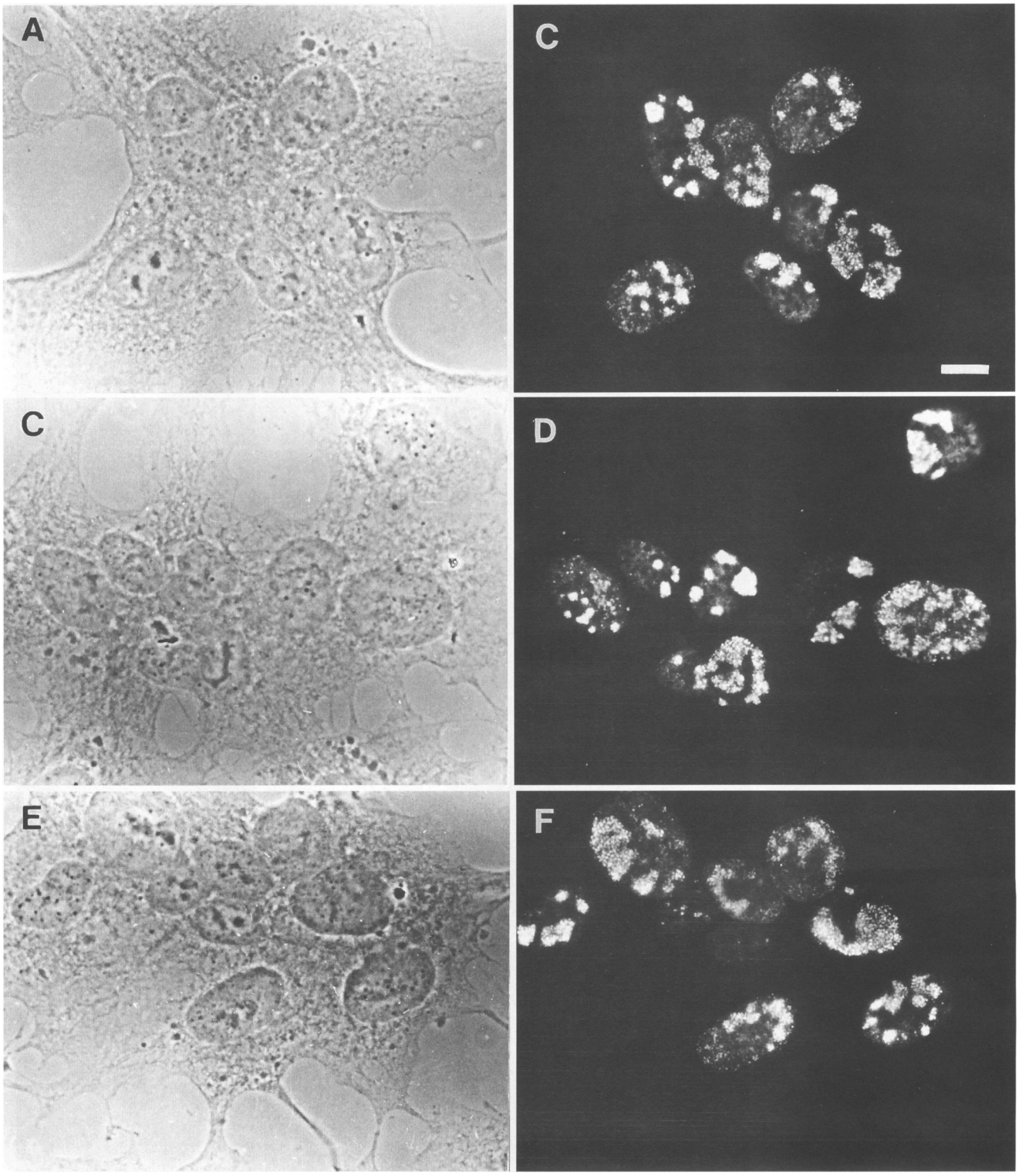


FIG. 10. Replication compartments in cells infected with a syncytial HSV strain. CV-1 cells were infected with the syncytium-forming macroplaque (MP) strain of HSV. Cells were fixed at 6 hpi and permeabilized as described in the legend to Fig. 1. Cells were stained with the 3-83 polyclonal antisera recognizing ICP8 followed by an FITC-conjugated goat anti-rabbit second antibody. Shown are phase-contrast (panels A, C, and E) and immunofluorescence (panels C, D, and F) micrographs of multinucleated cells. Bar, 10 μm.

e.g., DNA replication, late transcription, and encapsidation, could be important in production of progeny virus. Previous work has suggested a relationship between replication compartments and prereplicative sites (8, 27). It is possible that the substructures observed within replication compartments are equivalent to prereplicative sites; these sites could be dispersed when viral DNA replication is inhibited and grouped into functional viral replication domains when DNA replication is permitted. If this were the case, it would argue that spatial distribution of these structures is relevant to their function.

**HSV replication structures form within the context of preexisting nuclear architecture.** We examined the distribution of HSV DNA replication structures in binucleate cells to determine whether HSV DNA replication structures are assembled at random or specific sites in the cell nucleus. The examination of ICP8 staining patterns in binucleate cells revealed mirror image symmetry of replication compartments around a twofold axis running between sister nuclei. These symmetrical patterns most likely resulted from the infection of preexisting binucleate cells, as HSV infection did not increase the number of binucleate cells in the cultures. In addition, multinucleated cells that arose during infection with a syncytial HSV strain did not show symmetry among the nuclei. These results argue that preexisting structural elements in the paired nuclei of the binucleate cells determine the location and shape of the viral DNA replication compartments. Thus, the sites of a nuclear metabolic process, i.e., DNA replication, are defined by a nuclear structure that can be passed to daughter nuclei. Together with evidence for nonrandom chromosome arrangements in newly divided cells (22), these results indicate that a nuclear architecture, which can be transmitted to daughter cells, defines the location of both chromosomes and nuclear metabolic processes.

The formation of HSV DNA replication compartments within the context of preexisting nuclear spatial architecture implies that HSV DNA replication proteins are localized to specific regions in the infected cell nucleus. This may reflect targeting of the viral proteins to specific cell structures or molecules; alternatively, viral proteins may localize to areas where formation of replication compartments is not impeded by existing host structures. An example of a situation where viral proteins might localize to a site not impeded by host structures would be the formation of replication compartments at nuclear sites where there is no host chromatin. Nevertheless, as the replication compartments grow, they appear to be able to displace cellular chromatin to the periphery of the nucleus, causing the cytopathic effect called margination of host chromatin (17, 28). If viral proteins are targeted to specific domains in the nucleus on the basis of the presence of host nuclear structures, viral structures could be organized as a result of the association of ICP8 and/or other viral proteins with nuclear structural systems such as the nuclear matrix. Our findings that prereplicative sites and replication compartments are organized in the nuclear interior lead us to consider an internal matrix more likely than peripheral envelope structures to play such a role. If the nuclear matrix governs the formation of replication compartments in particular regions of the nucleus, this would imply regional differences in the nuclear matrix or associated proteins. Such regions could reflect microenvironments within the nucleus rich in cellular components necessary for specific processes such as DNA replication.

The observation that the host cell nuclear structure defines the site of assembly of viral replication structures raises the additional questions of the identity of the cellular nuclear receptor(s) for ICP8 and/or the other HSV DNA replication proteins and the order of their assembly into prereplicative sites. Analysis of mutant viruses defective for each of the HSV DNA replication proteins is being conducted to define their requirement for assembly of prereplicative sites and their order of incorporation into these structures.

An alternative model for the nonrandom distribution of replication compartments is that viral proteins may be localized to areas where the formation of viral compartments is not impeded by existing cellular structures. In this model, viral proteins would be localized by default to certain regions of the cell nucleus. As with the first scenario, this would argue that the structural architecture of the nucleus dictates the location of the viral structures. Regardless of which process occurs, our results argue strongly that an internal nuclear architecture duplicated in the daughter nuclei of binucleate cells defines the location at which viral DNA replication structures are assembled.

This study implies the existence of higher-level, heritable order in the nucleus. Examination of the distribution of antigens involved in a particular metabolic process in intact cells provides an alternative to use of extracted cells, where biochemical artifacts pose significant potential problems. The use of paired nuclei from binucleate cells, as exploited in this work, may provide a general test to determine whether nuclear components are localized to random structures or specific sites within the cell nucleus.

## ACKNOWLEDGMENTS

This work was supported by Public Health Service grant CA 26345. Confocal microscopy was performed at the facility in the Department of Anatomy and Cellular Biology, Harvard Medical School, which is supported by Public Health Service grant S10 RR04951.

We thank Karl Matlin and Marja Van Zeijl for advice on confocal microscopy, Joel Swanson for helpful discussion, and Brian Burke for the gift of the lamin antibody. We are indebted to Peter Daifuku for development of the software used for three-dimensional modeling and for useful discussions concerning three-dimensional computer graphics. We are grateful to Hewlett-Packard/Apollo for use of the DN10000 graphics workstation, the GMR3D rendering library, and peripheral equipment.

## REFERENCES

1. **Bush, M., D. Yager, M. Gao, K. Weisshart, A. Marcy, D. Coen, and D. Knipe.** 1991. Correct intranuclear localization of herpes simplex virus DNA polymerase requires the viral ICP8 DNA-binding protein. J. Virol. **65**:1082–1089.
2. **Cardoso, M. C., H. Leonhardt, and B. Nadal-Girard.** 1993. Reversal of terminal differentiation and control of DNA replication: cyclin A and Cdk2 specifically localize at subnuclear sites of DNA replication. Cell **74**:979–992.
3. **Carter, K. C., D. Bowman, W. Carrington, K. Fogarty, J. A. McNeil, F. S. Fay, and J. B. Lawrence.** 1993. A three-dimensional view of precursor messenger RNA metabolism within the mammalian nucleus. Science **259**:1330–1335.
4. **Challberg, M. D.** 1986. A method for identifying the viral genes required for herpesvirus DNA replication. Proc. Natl. Acad. Sci. USA **83**:9094–9098.
5. **Challberg, M. D., and T. J. Kelly.** 1989. Animal virus DNA replication. Annu. Rev. Biochem. **58**:671–717.
6. **Chen, L. B.** 1993. Personal communication.
7. **Darlington, R. W., and C. James.** 1966. Biological and morphological aspects of the growth of equine abortion virus. J. Virol. **92**:250–257.
8. **de Bruyn Kops, A., and D. M. Knipe.** 1988. Formation of DNA replication structures in herpes virus-infected cells requires a viral DNA binding protein. Cell **55**:857–868.
9. **de Bruyn Kops, A., and D. M. Knipe.** Unpublished data.
10. **Foley, J., A. van Dam, S. Finer, and J. Hughes.** 1990. Computer

graphics principles and practice, 2nd ed. Addison Wesley Publishing Co., Reading, Mass.
11. **Gao, M., and D. M. Knipe.** 1992. Distal protein sequences can affect the function of a nuclear localization signal. Mol. Cell. Biol. **12:**1330–1339.
12. **Gibson, S. F., and F. Lanni.** 1991. Experimental test of an analytical model of aberration in an oil-immersion objective lens used in three-dimensional light microscopy. J. Opt. Soc. Am. **8:**1601–1613.
13. **Goodrich, L. D., P. A. Schaffer, D. I. Dorsky, C. S. Crumpacker, and D. S. Parris.** 1990. Localization of the herpes simplex virus type 1 65-kilodalton DNA-binding protein and DNA polymerase in the presence and absence of viral DNA synthesis. J. Virol. **64:**5738–5749.
14. **Hoggan, M., and B. Roizman.** 1959. The isolation and properties of a variant of herpes simplex producing multinucleated giant cells in monolayer cultures in the presence of antibody. Am. J. Hyg. **70:**208–219.
15. **Huberman, J., A. Tsai, and R. Deich.** 1973. DNA replication sites within nuclei of mammalian cells. Mol. Cell. Biol. **241:**32–36.
16. **Hughes, R. G., Jr., and W. H. Munyon.** 1975. Temperature-sensitive mutants of herpes simplex virus type 1 defective in lysis but not in transformation. J. Virol. **16:**275–283.
17. **Knipe, D. M.** 1989. The role of viral and cellular nuclear proteins in herpes simplex virus replication. Adv. Virus Res. **37:**85–123.
18. **Knipe, D. M.** 1990. Virus-host cell interactions, p. 293–316. *In* B. N. Fields and D. M. Knipe (ed.), Virology, 2nd ed. Raven Press, New York.
19. **Knipe, D. M., D. Senechek, S. Rice, and J. Smith.** 1987. Stages in the nuclear association of the herpes simplex virus transcriptional activator protein ICP4. J. Virol. **61:**276–284.
20. **Knipe, D. M., and A. Spang.** 1982. Definition of a series of stages in the association of two herpesviral proteins with the cell nucleus. J. Virol. **43:**314–324.
21. **Lehner, C., V. Kurer, H. Eppenberger, and E. Nigg.** 1986. The nuclear lamin protein family in higher vertebrates: identification of quantitatively minor lamin proteins by monoclonal antibodies. J. Biol. Chem. **261:**13293–13301.
22. **Locke, M.** 1990. Is there somatic inheritance of intracellular patterns? J. Cell Sci. **96:**563–567.
23. **Lorenson, W., and H. Cline.** 1987. Marching cubes: a high resolution 3D surface construction algorithm. Comput. Graphics **21:**163–169.
24. **Mao, J., and E. Robishaw.** 1975. Mode of inhibition of herpes simplex virus DNA polymerase by phosphonoacetate. Biochemistry **14:**5475–5479.
25. **Moen, P. T., Jr., E. Fox, and J. W. Bodnar.** 1990. Adenovirus and minute virus of mice DNAs are localized at the nuclear periphery. Nucleic Acids Res. **18:**513–520.
26. **Olivo, P. D., N. J. Nelson, and M. D. Challberg.** 1989. Herpes simplex virus type 1 gene products required for DNA replication: identification and overexpression. J. Virol. **63:**196–204.
27. **Quinlan, M., L. B. Chen, and D. Knipe.** 1984. The intranuclear location of a herpes simplex virus DNA binding protein is determined by the status of viral DNA replication. Cell **36:**857–868.
28. **Randall, R. E., and N. Dinwoodie.** 1986. Intranuclear localization of herpes simplex virus immediate-early and delayed-early proteins: evidence that ICP4 is associated with progeny virus DNA. J. Gen. Virol. **67:**2163–2177.
29. **Rixon, F. J., M. Atkinson, and J. Hay.** 1983. Intranuclear distribution of herpes simplex virus type 2 DNA synthesis: examination by light and electron microscopy. J. Gen. Virol. **64:**2087–2092.
30. **Roizman, B., and A. E. Sears.** 1990. Amplification by host cell factors of a sequence contained within the herpes simplex virus 1 genome. Proc. Natl. Acad. Sci. USA **87:**9441–9444.
31. **Schwartz, J., and B. Roizman.** 1969. Similarities and differences in the development of laboratory strains and freshly isolated strains of herpes simplex virus in HEp-2 cells: electron microscopy. J. Virol. **4:**879–889.
32. **Shuman, H., J. Murray, and C. DiLullo.** 1989. Confocal microscopy: an overview. BioTechniques **7:**154–163.
33. **Voelkerding, K., and D. F. Klessig.** 1986. Identification of two nuclear subclasses of the adenovirus type 5-encoded DNA-binding protein. J. Virol. **60:**353–362.
34. **Weller, S. K.** 1991. Genetic analysis of HSV-1 genes required for genome replication, p. 105–136. *In* E. K. Wagner (ed.), Herpesvirus transcription and its regulation. CRC Press, Baton Rouge, La.
35. **Wilcock, D., and D. Lane.** 1991. Localisation of p53, retinoblastoma and host replication proteins at sites of viral replication in herpes-infected cells. Nature (London) **349:**429–431.
36. **Wu, C. A., N. J. Nelson, D. J. McGeoch, and M. D. Challberg.** 1988. Identification of herpes simplex virus type 1 genes required for origin-dependent DNA synthesis. J. Virol. **62:**435–443.